



Eco-friendly modified engineered cementitious composites: a study on mechanical, durability and microstructure characteristics

N. Shanmugasundaram · S. Praveenkumar

Received: 16 February 2024 / Accepted: 9 June 2024 / Published online: 15 June 2024
© The Author(s), under exclusive licence to RILEM 2024

Abstract This research examined the development of modified engineered cementitious composites (MECC) using manufactured sand (M-sand) and a high content of raw agricultural by-products, such as bagasse ash (BA) and rice husk ash (RHA), instead of conventional silica sand and fly ash. Fourteen different types of MECC mixtures were developed using raw BA and RHA blended with M-sand to reduce the cost of MECC. The fresh and hardened properties of all mixtures were examined using various types of testing methods. In addition, microstructure analysis were conducted for both the control and optimal mixtures to identify the bonding of fibres in cementitious composites. The correlation between conventional and MECC was also evaluated based on the hardened properties and cost analysis. The results revealed that workability steadily dwindled with increasing percentages of BA and RHA, from 10 to 55. Optimal mechanical properties were attained with the incorporation of BA and RHA at 10% cement replacement. In contrast, 30% BA and 40% RHA exhibited maximum

impact strength compared to the respective control mixes. Similarly, ECC with 20% BA and RHA exhibited optimal durability properties. Moreover, compared to conventional ECC, the cost of the newly developed MECC was slightly lesser due to the incorporation of agricultural by-products and M-sand.

Keywords Engineered cementitious composites · Bagasse ash · Rice husk ash · M-sand · Fresh and hardened properties

1 Introduction

The replacement of cement with agricultural and industrial by-products has received attention for various civil engineering applications in recent years, owing to its pozzolanic characteristics. Specifically, many researchers have successfully used agricultural by-products, namely bagasse ash and rice husk ash, as pozzolans in cement composites. The use of these by-products in cement as supplementary cementitious materials (SCM) helps to minimize the global warming due to greenhouse gases emission from cement industries and the disposal of agricultural and industrial waste ashes [1, 2]. Both BA and RHA are residual waste ashes from agro-based industries that contain amorphous silica, which acts as a pozzolanic material in cement replacement. The presence of high silica in these ashes reacts with calcium and forms the C_2S during hydration process, which helps

N. Shanmugasundaram
Advanced Concrete Research Laboratory, Department
of Civil Engineering, PSG College of Technology,
Coimbatore, India
e-mail: shancivilguy@gmail.com

S. Praveenkumar (✉)
Department of Civil Engineering, PSG College
of Technology, Coimbatore, India
e-mail: spk.civil@psgtech.ac.in



to attain the strength of concrete at later ages [3, 4]. Similarly, the presence of small amounts of other oxide compounds such as alumina, calcium, and iron in RHA and BA also contributes to cement hydration. In addition, it is proved that the proposed SCM's increases the formation of calcium silicate hydrate (C-S-H) gel, which intern increases the density of the mix and thereby reduces the pore diameter around the cement particles [5–7].

On the other hand, the development and use of Engineered Cementitious Composite (ECC) in various applications significantly increased all over the world owing to its tensile strain-hardening behavior, which is contrary to the quasi-brittle nature of fibre reinforced concrete (FRC) [8–10]. Many investigators have attained a ultimate tensile strength, strain and flexural strength of ECC from 4–12 MPa, 1–8% and 10–30 MPa. Similarly, the compressive strength, modulus of elasticity and density of ECC varies from 20–95 MPa, 18–34 GPa and 0.95 to 2.3 g/cm³ [11]. However, the inclusion of different fine aggregates, fibres and SCMs, affects the various properties of ECC. Hence, the application of ECC is differed based on these properties, i.e., repair and rehabilitation works, earthquake resistance structures, precast construction, high-pressure pipelines, coastal structures, bridge structures, etc. [12]. Also, the higher percentage of cement replacement (1:1.2 or 2.2) by SCMs in ECC reduces the usage of cement, thereby decreasing the emission of CO₂ gases, construction costs, and land, air, and water pollution [13, 14].

Subedi et al. [15] attained higher surface resistivity, first cracking and tensile strength of ECC with the inclusion of post-processed BA instead of fly ash (FA). Compared to FA, BA increases the fibre matrix chemical bond and fracture toughness matrix, which increases the strength of the ECC. However, decreasing trends of ductility and compressive strength were observed when the replacement of cement was increased by more than 25%. Furthermore, using an excess of BA considerably lowers the workability of the mixtures and prevents effective fibre dispersion. The fibre-bridging ability was increased with the incorporation of 50% BA, where it was decreased at 60% of cement replacement owing to poor workability [16]. Similarly, 10% BA in ECC exhibited optimal compressive, tensile, and flexural strengths at 28 days. However, decreasing

trends were observed at 3 and 7 days owing to insufficient or no pozzolanic action in the early phases. Also, a positive impact was observed in ECC with the incorporation of processed BA compared to raw BA due to the improvement of physical properties [17].

On the other side, Zhang et al. [18] evolved the eco-friendly ECC with the inclusion of RHA as FA replacement. Replacing FA with RHA enhanced the hydration rate, pozzolanic reaction and strengthened the pore size distribution in the composites, which dramatically increased the compressive strength by approximately 31.707%. Moreover, the development of ECC necessitates the use of silica sand, which increases the demand for the material's inherent environmental and energy footprints, along with the scarcity of high-quality produced silica sand [19]. Meanwhile, the use of manufactured sand (M-sand) has been promoted in the research and construction sectors over the past decade because of the increasing cost and demand of conventional silica sand and river sand [20]. Based on the above findings from various studies, M-sand was used as a fine aggregate in this research without compromising the strength and other parameters instead of silica sand. Furthermore, the cement was replaced with raw BA and RHA from 0 to 55% for the development of MECC. The ECC performance was determined using a flow table, compressive strength, direct tensile strength and strain, flexural strength, impact test, and rapid chloride permeability test (RCPT). In addition, the bonding of the fibres were analyzed using SEM analysis. Mechanical characteristics and cost-benefit analyses were also conducted for conventional and MECC.

2 Research significance

In the last two decades, the application of ECC has been extended worldwide owing to its immense strain-hardening behavior, and the inclusion of conventional SCM, fine aggregates, fibres and other locally available by-products. Many researchers have examined the mechanical properties of ECC with various SCM such as GGBS, FA, silica fume and metakaolin blended with silica sand. In this study, a novel and sustainable MECC was developed using



BA, RHA, and M-sand. Moreover, the following essential questions were addressed in this study.

- Is BA and RHA enhanced the strain-hardening behavior of ECC rather than conventional one?
- Does different w/cm ratios and specific mixing methods enrich the fibre diffusion and homogeneity of mixes?
- How do the fresh, mechanical and durability properties of the proposed MECC differ from those of the conventional ECC?
- Based on the applications and strength parameters, what is the optimal percentage of agricultural by-products that can be used for ECC development?

3 Materials and methodology

In this research, Ordinary Portland cement (OPC-53 grade) was used according to the recommendation of IS 12269-1987. The agricultural by-products, BA and RHA, were collected from a rice mill and a natural brown sugar processing plant in Erode, Tamil Nadu. The physical and chemical properties of the binders are listed in Table 1 and 2, respectively. The blain's specific surface area and specific gravity of BA and RHA attained 203.6 m²/kg and 243.7 m²/kg, and 2.334 and 2.062, respectively. In addition, the strength activity index (SAI) of BA and RHA attained above 75%, as recommended by ASTM C311-11b. Higher amount of SiO₂ is present in the BA and RHA than in

OPC. The total amounts of SiO₂ + Al₂O₃ + Fe₂O₃ in the OPC, BA, and RHA were 21.874%, 62.303%, and 96.131%, respectively. The particle size distribution of the binders and the morphological investigation of BA and RHA are illustrated in Figs. 1 and 2, respectively. From the morphology study, it was noted that the ash samples were composed of voids with different sizes and geometries. Notably, higher amounts of round and elongated particles were observed in BA than in RHA. However, large amounts of fine and irregular materials were observed in the RHA sample. Zone II manufactured sand with a relative density of 2.64, fineness modulus of 2.71, and water absorption of 1.12% was used as fine aggregates in this study. Polyvinyl alcohol (PVA) fibres with an aspect ratio of 307.67 and a tensile strength of 1600 MPa were used. The physical properties of the fibres are listed in Table 3. In addition, laboratory tap water and a polycarboxylate ether-based high-range water reducer (Auramix 400) were used.

4 Mixing method and mix proportions

To achieve complete dispersion of fibres with cement composites, the mixing procedure was meticulously planned for 20 min using a high-speed planetary mixer. Initially, binders such as OPC and BA/RHA were mixed thoroughly in a dry state for approximately 3 min at an average speed. Subsequently, M-sand was incorporated into the dry mix, and the mix was continued for an additional two min to

Table 1 Physical properties of binders

Properties	OPC	BA	RHA	Code recommendation	Standards
Specific surface area (m ² /kg)	343	203.6	243.7	≥ 300	IS 4031-2 (1996)
Specific gravity	3.164	2.334	2.062	Nearly 3.15	IS 4031-11 (1988)
Compressive strength (MPa)	53.37	-	-	≥ 53	IS 4031-11 (1988)
SAI at 7 days (%)	100	89.39	79.91	> 75	ASTM C311-11b
SAI at 28 days (%)	100	77.23	78.45		

Table 2 Chemical composition of binders

Composition	CaO	SiO ₂	Al ₂ O ₃	MgO	P ₂ O ₅	Fe ₂ O ₃	K ₂ O	TiO ₂	SO ₃	MnO	SiO ₂ + Al ₂ O ₃ + Fe ₂ O ₃
OPC	68.97	15.61	3.24	2.19	0.38	6.01	1.00	0.29	4.14	0.10	24.874
BA	9.59	52.60	4.89	2.25	5.66	4.80	13.5	0.52	8.21	0.11	62.303
RHA	0.9	95.85	0.01	0.12	1.04	0.26	1.57	0.02	0.08	0.00	96.131

Fig. 1 Particle size distribution of cement and binders

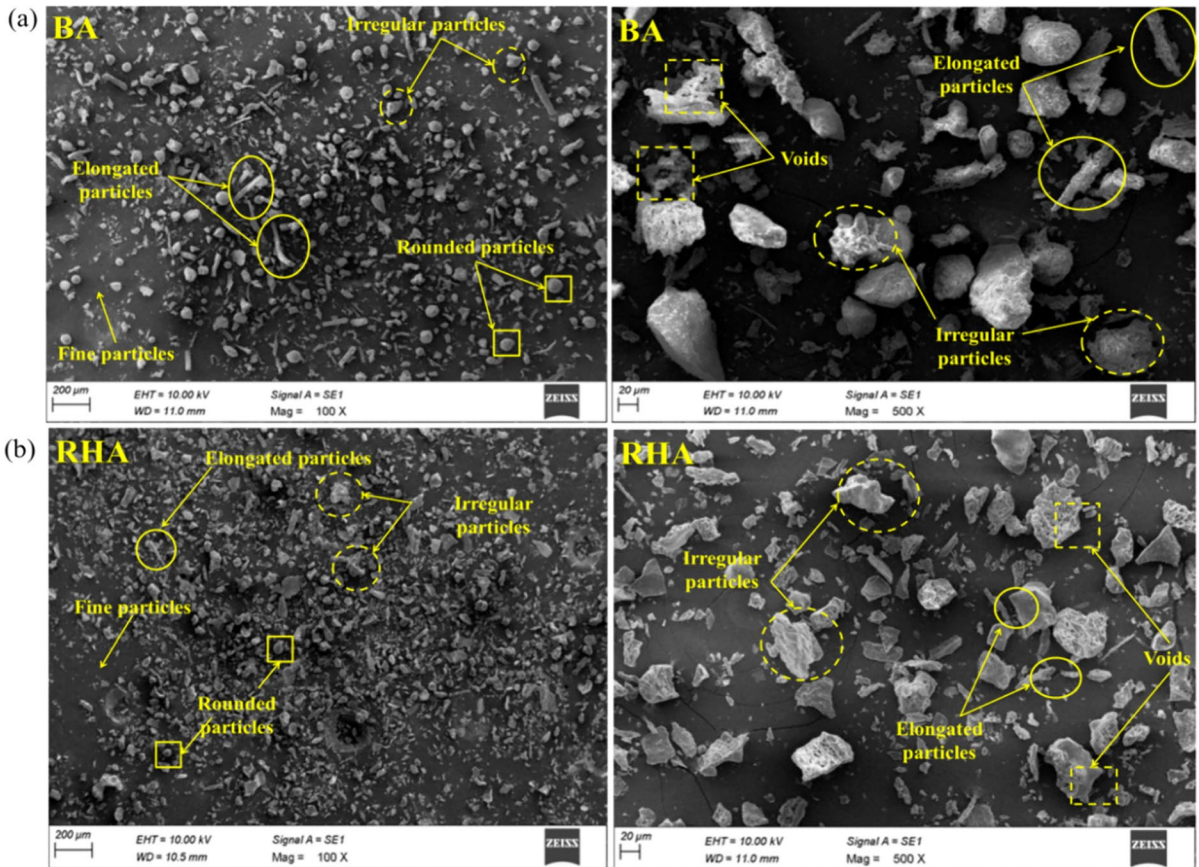
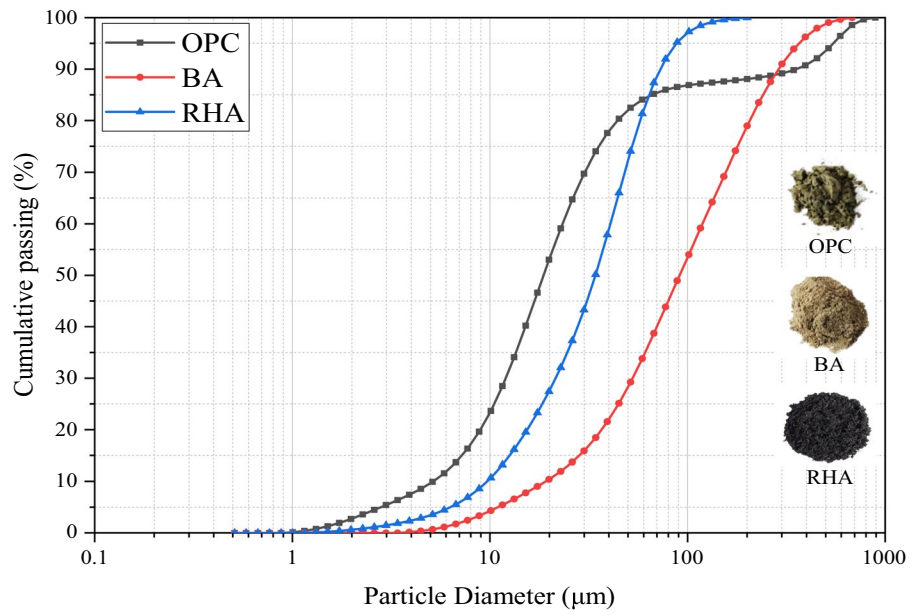


Fig. 2 SEM image of agricultural by-products: **a** Bagasse ash and **b** Rice husk ash



Table 3 Properties of PVA fibre

Length (mm)	Diameter (μm)	Tensile strength (MPa)	Modulus of elasticity (GPa)	Density (kg/m^3)	Elongation (%)	Aspect ratio
12	39	1600	42.8	1300	6	307.67

achieve homogeneity. Further, the PVA fibres were slowly added to the dry matrix and the mix was carried out for approximately 10 min (8 min slow and 2 min fast). Finally, the water and (high range water reducer) HRWR were slowly added to the dry matrix, and the mixing was continued for 3 min slower and 2 min faster, respectively, to achieve proper liquefaction. The standard mix design procedure was not recommended by V.C.Li for the development of ECC owing to the incorporation of various materials. Hence, it was achieved based on a series of trial mixes to achieve better performance in regard to the fresh and hardened properties. In this study, the mix proportions were categorized with two w/c ratios such as 0.36 and 0.37 for BA and RHA mixes. The fine aggregate and PVA fibres were kept constant in all the mixes. The HRWR was modified to all BA and RHA-blended ECC mixes in accordance with the flow value observed in the respective control mixes (CM).

The mix without agricultural by-products was kept as a CM, which was labeled as CM 0.36 and CM 0.37, respectively. In this study, OPC was replaced separately with BA and RHA at different percentages

(10, 20, 30, 40, 50, and 55). In Table 4, the separate Mix ID is given for all ECC with BA and RHA; that is, 10BA denotes that OPC was replaced with 10% BA. Similarly, 40RHA indicates that OPC was replaced with 40% RHA.

5 Testing methods

To ensure the fibre distribution and thereby enhance the properties of ECC, the flow percentage were determined by a flow table test according to IS 5512 (1983). The average flow was calculated from six directions, and the HRWR was added in each mix to attain the flow value of the corresponding CM. The compressive strength was measured using 70.6 mm cube specimens at 3, 7 and 28 days according to IS:4031-6 (1988). The direct tensile properties were determined using dog-bone specimens according to JSCE.

The flexural test was conducted using a flexural jig assembly with a specimen size of 160 mm \times 40 mm \times 40 mm, as recommended by ASTM C109 (2016). Furthermore, the impact test of

Table 4 Mix proportions (kg/m^3)

Group	Mix ID	Cement	Agricultural by-products	Fine aggregate	Fibre	W/CM	HRWR
Group-BA	CM 0.36	1254	0	456	26	0.36	0
	10BA	1129	125				0.878
	20BA	1003	251				2.006
	30BA	878	376				3.511
	40BA	752	502				5.016
	50BA	627	627				7.148
	55BA	564	690				8.778
Group-RHA	CM 0.37	1254	0	456	26	0.37	0
	10RHA	1129	125				1.254
	20RHA	1003	251				2.633
	30RHA	878	376				4.264
	40RHA	752	502				6.772
	50RHA	627	627				9.029
	55RHA	564	690				10.032

ECC was performed with a specimen size of 152 mm dia and 62.5 mm thickness according to ACI 544.5R-10. RCPT was carried out on the specimens (100 mm diameter and 50 mm thickness) at the age of 28 and 90 days, respectively, according to ASTM C 1202. This test was carried out to assess the electrical conductance and provide a rapid assessment of their resistance to penetration of chloride ion into the samples. The SEM analysis was conducted to study the fibre-bridging effect for the control and optimal mixtures of both BA and RHA samples using the core of the samples (6 mm × 6 mm × 4 mm).

6 Results and discussion

6.1 Fresh property

The flow percentage of ECC blended with BA and RHA is shown in Fig. 3. The flow was significantly reduced by replacing the OPC with different percentages of BA and RHA. Mixtures CM 0.36 and CM 0.37 reached the flow percentages of 91.2 and 92.5,

respectively. However, these flow percentages progressively decreased with increasing percentages of BA and RHA, from 10 to 55. The mix CM 0.37 attained a higher flow than CM 0.36 owing to the high water content, which also increased the fibre diffusion of the mixes. Nevertheless, lower cement content and the presence of voids and irregular shapes in both BA and RHA increase the water demand in the mixes, negatively impacting flowability. Interestingly, the flow of ECC blended with BA increased slightly compared to that of the RHA mixes. It is possibly due to the high quantities of rounded particles presences in the BA, as shown in Fig. 2. These rounded particles in BA exhibit smoother surfaces compared to irregular shapes. Consequently, less friction is developed during mixing; this reduced friction promotes smoother movement and redistribution of particles within the mixture, thereby increasing flowability. A similar trend of outcomes was also observed in earlier studies [16] where increasing the percentage of BA and RHA in ECC decreased the flowability.

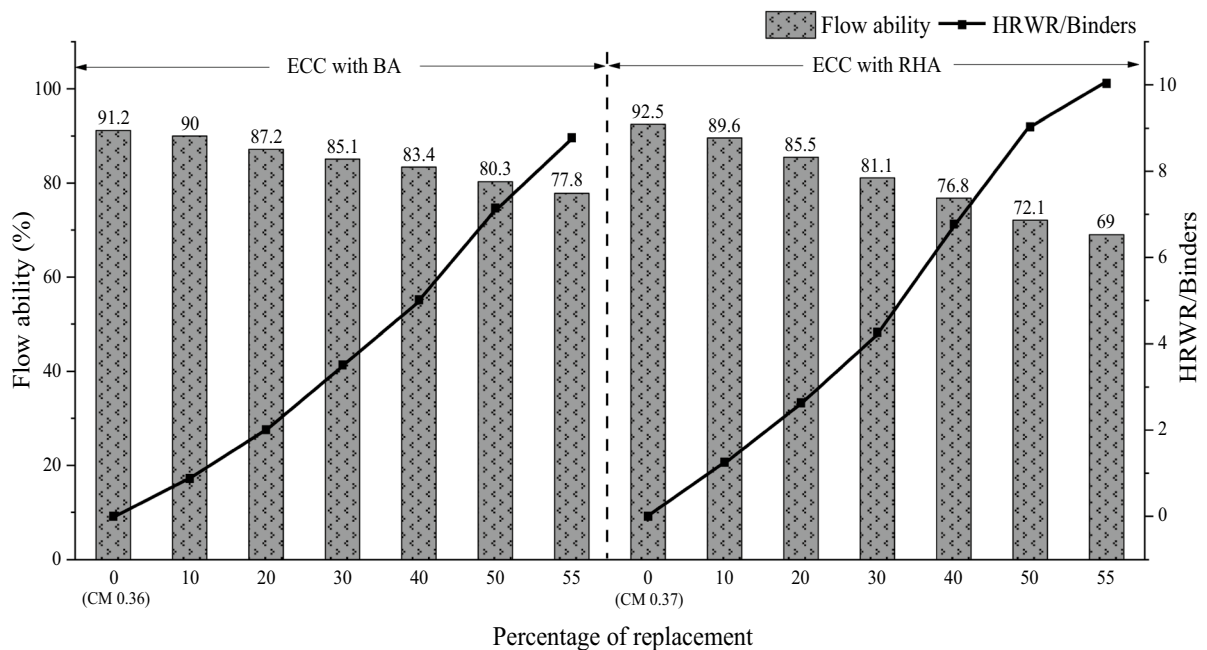


Fig. 3 Flow ability of BA and RHA blended ECC



6.2 Mechanical properties

6.2.1 Compressive strength

Compressive strength of ECC blended with different proportions of BA and RHA at 3, 7 and 28 days is shown in Fig. 4. The mix 10BA exhibits high strength of about 54.12 MPa at 28 days of testing, which is 1.844% marginally higher than CM 0.36. However, the addition of more BA affected a gradual decrease in the early and later strengths of mixes 20BA, 30BA, 40BA, and 50BA, respectively. Less pozzolanic action in the early phases in all BA blended mixes was the reason for strength loss. Nevertheless, this trend of reduction in strength with an increasing percentage of BA was entirely reversed by extending the testing age (28 days). The total quantities of $\text{SiO}_2 + \text{Al}_2\text{O}_3 + \text{Fe}_2\text{O}_3$ were higher in BA (62.303%) than in OPC (24.874), which contributed to enhancing the secondary hydration and thereby increasing the strength at a later age. A similar trend of strength diminishing at 3 and 7 days and then improving at 28 days was also observed in the various research [17,

21]. The strength of 55BA decreased considerably at early and later ages compared to other ECC mixes blended with BA. However, it reached a strength of above 40 MPa at a later age, which attains the minimum strength requirement for various applications according to ACI 318. The decrease in cement percentage has a negative impact on the cement hydration, voids, and porosity of ECC, along with its strength properties at different ages. In particular, the cement hydration decreased in the mixes at early and later ages when the cement was replaced with BA owing to the lower cement content. This phenomenon is called the dilution effect, and it is a reason for the strength reduction in mixes 20BA to 55BA. Conversely, the later strength of 30BA slightly increased with a percentage of 0.613 compared to 20BA. The particular particle sizes of BA contribute to improved particle packing in composites due to adequate water content. This reduction in voids consequently enhances the strength of the 30BA [22–24].

A related outcome of ECC with BA has been observed in ECC with RHA. The mix 10RHA attained the high compressive strength of 26.24 MPa,

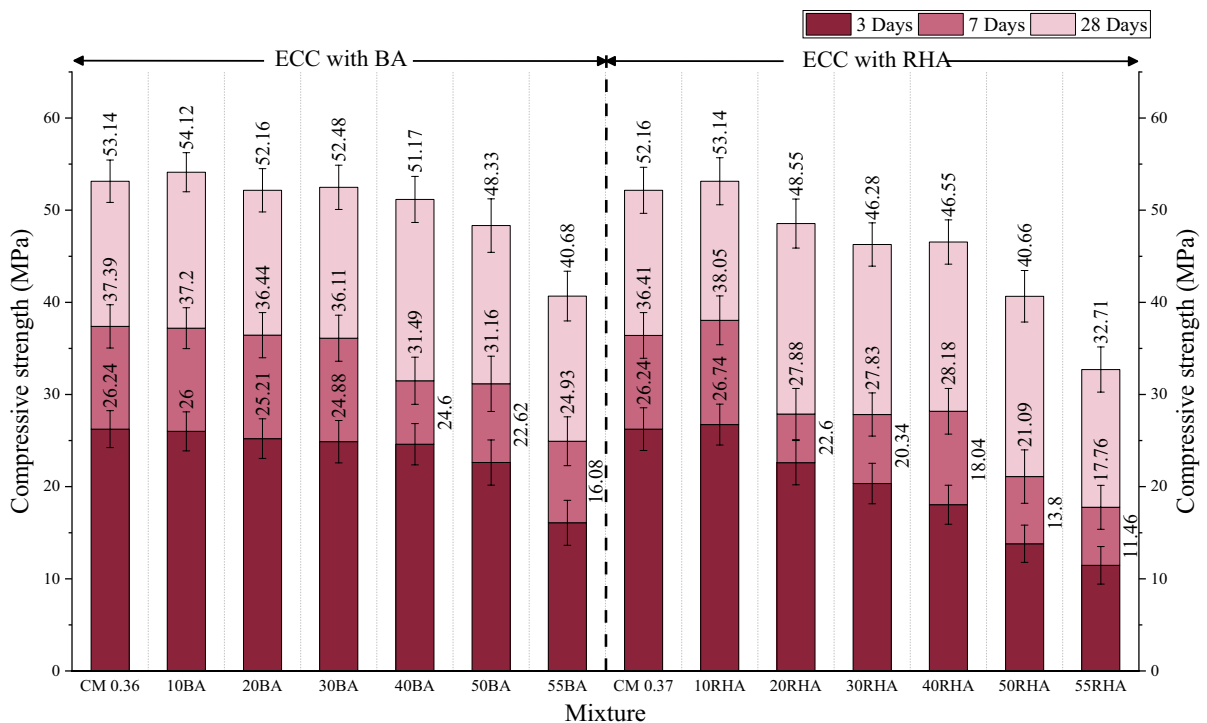


Fig. 4 Compressive strength of BA and RHA blended ECC



38.05 MPa and 53.14 MPa at different ages of testing (i.e. 3, 7 and 28), which are comparably 1.905%, 4.504% and 1.878% higher than the corresponding CM 0.37. Compared to CM 0.37, the strength of 10RHA increased because of the micro-filler effect and high pozzolanic reaction of RHA. A significantly dense matrix was developed by RHA as a result of the microfiller effect, which distributes C-S-H more uniformly in the composites. Furthermore, the elevated silica content (95.85%) in RHA led to a substantial formation of C-S-H gel during secondary hydration, contributing to an enhanced dense microstructure matrix. Typically employed as a binder in cement, RHA exhibits a microporous geometry with an amorphous silica composition ranging from 80 to 95%. This amorphous silica possesses the potential to engage with calcium hydroxide crystals formed during the hydration process, leading to additional C-S-H gel formation. This, in turn, aids in filling the voids within the ECC mixes. Also, RHA reduces the voids between cement particles, thereby indirectly strengthening the interlocking of the entire mix. Consequently, composites with greater densities and strengths were produced. These findings concur with those of Khan et al. [25] and da Costa et al. [26], who identified a decrease in the strength of ECC when OPC was replaced by high percentage of RHA. In contrast, the 7 and 28 days strength of 40RHA was

slightly increased to 1.25% and 0.583% compared to 30RHA. This is probably because the adequate water in the mixes enriches the fibres dispersion and homogeneity of the mixes, which can enhance the strength by preventing the formation of cracks in the ECC.

6.2.2 Direct tensile properties

The direct tensile properties of the ECC blended with BA and the corresponding crack development is illustrated in Fig. 5. The failure of all mixes occurred at different points in the gauge length of the dog-bone specimen. In addition, using BA as a replacement for a particular percentage of cement exerts a considerable influence on tensile strength. The tensile strength of all the mixes attained similar results to the compressive strength. The 10BA mixture achieved the highest tensile strength at 2.826 MPa, surpassing other mixes. Nevertheless, increases in BA percentage over 10% led to a downtrend in tensile strength compared to CM 0.36. According to Subedi et al., [15] the frictional and chemical bonds between PVA fibre and a some proportion of BA will increase owing to the homogeneity of fibre diffusion in the mix. Therefore, this enhanced fibre matrix improves the bonding properties, which helps to attain a high tensile strength of the mixes. Contrary, owing to the

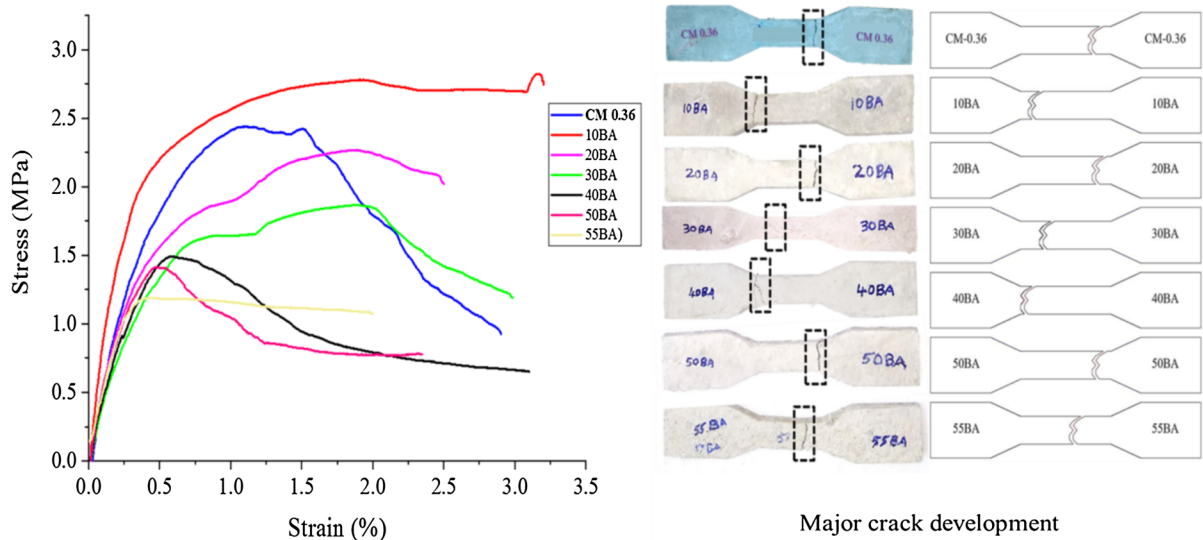


Fig. 5 Tensile property and major crack development of ECC blended with BA



high content of BA in other mixes (20BA—55BA) causes to led to dilution effect and also develops the water demand; accordingly reduction in fibre matrix and thereby tensile strength of ECC was decreased. In contrast, the strain of mixes 10BA, 30BA and 40BA slightly increased by 3.445%, 2.855% and 6.825% compared to CM 0.36. However, decreasing trends of strain were observed in 20BA, 50BA, and 55BA compared to CM 0.36. Nevertheless, ECC with BA revealed a tensile strain capacity approximately 250 times higher than that of conventional concrete (0.01%). It is well known that the fibre-bridging relationship (J_b') is a crucial factor in the ductility of ECC [27].

The fibres break in the pullout stage owing to an increase in the chemical bond between the fibre and matrix, which causes negatively impacts the J_b' and thereby decreases the ductility of 20BA, 50BA, and 55BA. Further, due to the homogeneity and binding of materials, the fibre bridging ability of the mixes 10BA, 20BA and 30BA were slightly increased and thereby improves the ductility of ECC, which was also discussed in Sect. 6.2.1. According to Tahmouresi et al. [28] and Fu et al. [29], improving the chemical bond in the fibre matrix and the toughness of the fibres increased the first-cracking strength, which increased the ductility of the mixes. The direct tensile properties of the ECC blended with RHA and the corresponding crack development is illustrated

in Fig. 6. The failure of all mixes occurred at the gauge length of the dog-bone specimens. Also, Fig. 6 shows that the addition of 10% RHA (10RHA) in ECC enhances the tensile strength from 2.165 MPa (CM 0.37) to 2.399 MPa, which is comparatively 10.80% higher than CM 0.37. However, increases in RHA content above 10% led to a reduction in strength similar to BA mixes. Whereas, the enhancement of tensile strain was observed in 10RHA, 30RHA and 40RHA in the percentage of 11.55, 2.325 and 6.94, respectively. At the same time, the strain of 20RHA, 50RHA and 55RHA was decreased to 6.54%, 6.01% and 23.98%, respectively compared to CM 0.37. The tensile strength of mixes 20RHA to 55RHA was considerably decreased by the increased RHA percentage due to the dilution effect. Also, the water demand of 20RHA to 55RHA blended mixes was increased due to less specific volume of RHA, which decreases the J_b' and matrix toughness (J_{tip}) and thereby decreases the tensile strength in ECC. A similar trend of the direct tensile strength diminishing of ECC with the incorporation of SCM was also observed in different studies [30].

6.2.3 Flexural strength

The variations in the flexural strength of BA and RHA blended ECC on different days (i.e., 3, 7, and 28) is illustrated in Fig. 7. The results for the flexural

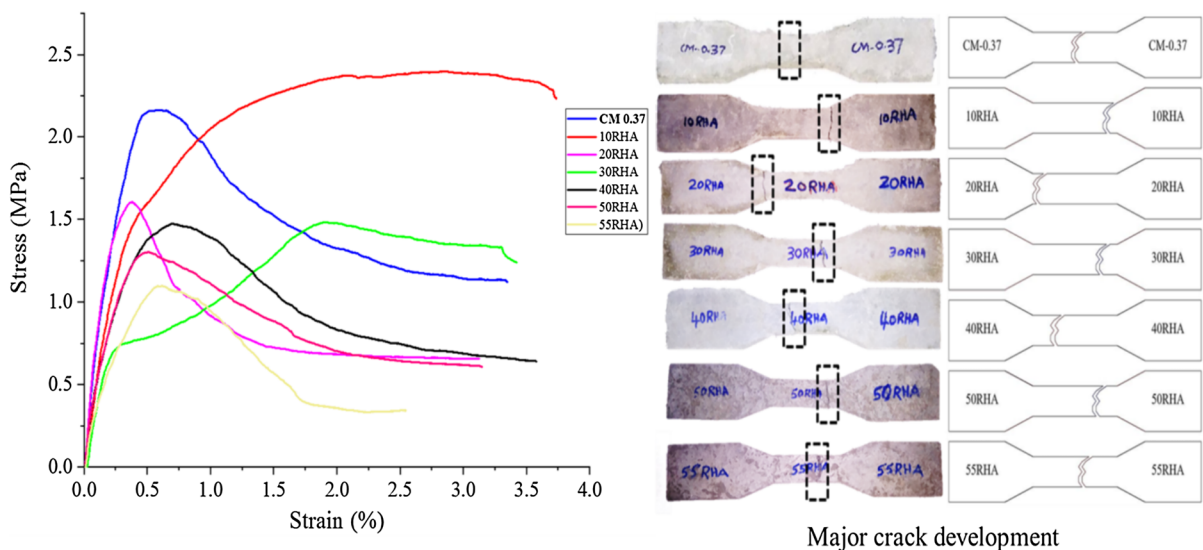


Fig. 6 Tensile property and crack development of ECC blended with RHA

strength of all mixes were almost similar to those for the compressive and tensile strengths. The maximum strength of 40.4 MPa, 43.21 MPa and 46.33 MPa was attained by 10BA at different ages. Nonetheless, decreasing trends of flexural strength occurred in 20BA to 55BA at all ages of testing. However, the 3 and 7 day strength of 20BA, 30BA and 40BA was slightly greater to CM 0.36. Also, the 3, 7 and 28 days of each mix was not increased dramatically except 55BA, and the minimum strength of 25.58 MPa, 33.54 MPa and 37.13 MPa was reached by 55BA at different ages of testing. The results show that incorporating 10% BA and a high aspect ratio of PVA fibre significantly improves flexural strength because of its fibrous character [30]. Also, as per the previous discussion on tensile properties, the use of BA specifically increased the J_b'/J_{tip} value, enhancing the flexural strength of the mixes. Similarly, maintaining sufficient workability in the mixes through specific mixing methods improves fibre diffusion, thereby contributing to a reduction in crack propagation during testing and ultimately improving the flexural strength [31]. The chemical bond between the fibres and binders was weakened owing to the high content of BA and less cement, which caused a

reduction in flexural strength. However, high bridging property attempts to arrest further crack development in the composites during loading, which increases the flexural strength. Furthermore, the 28 days strength was not significantly improved compared to 3 and 7 days in all mixes including CM 0.37. Previous studies have clearly proven that the fibre matrix, bridging, and bonding ability of composites contribute to their tensile and ductile properties [18]. Replacing OPC with RHA from 20 to 55% in ECC resulted in a lower flexural strength at all ages of testing, as illustrated in Fig. 7.

The maximum strength reached by 10RHA is about 43.52 MPa, 51.64 MPa and 54.6 MPa at 3, 7 and 28 days. While increasing the RHA content from 20 to 55% the strength was decreased from 30.11 MPa to 10.3 MPa, 38.53 MPa to 10.76 MPa and 43.99 MPa to 16.69 MPa at 3, 7 and 28 days. The mix 55RHA attained a minimum flexural strength of 10.3 MPa, 10.76 MPa and 16.69 MPa. It is known that the enhancement can be the result of increased friction between the fibre matrix owing to the better gradation of fine aggregates and the presence of a highly amorphous silica composition in RHA [25]. However, this fibre matrix weakened owing

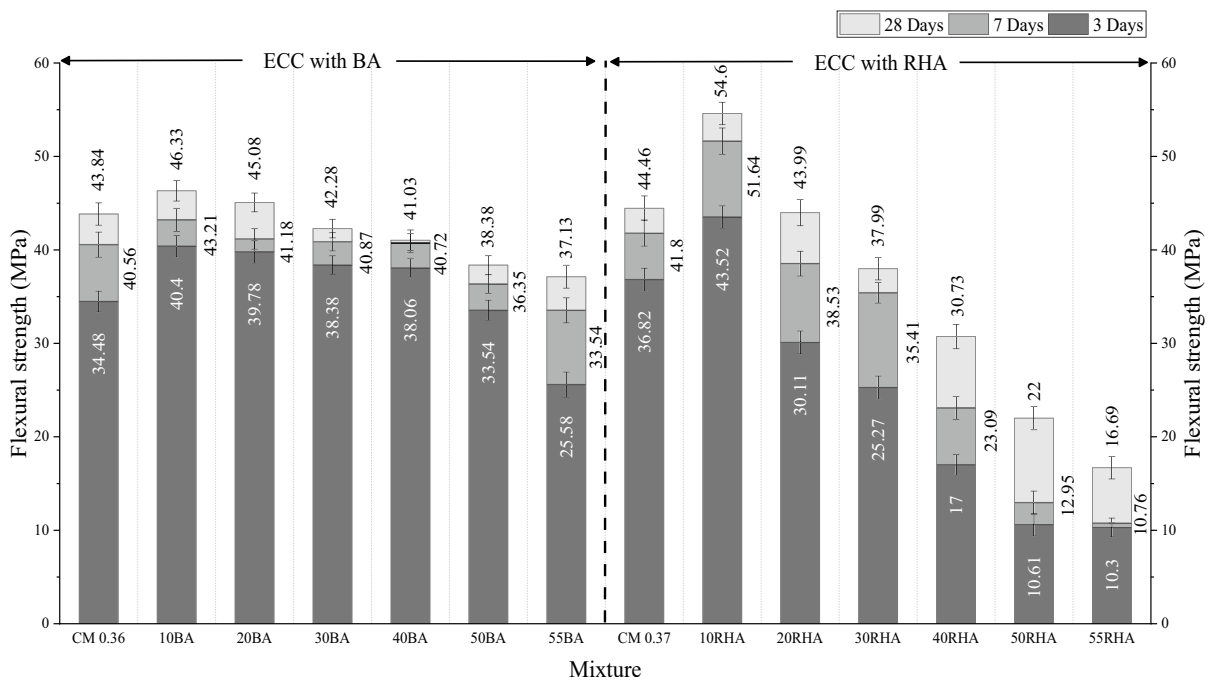


Fig. 7 Flexural strength of BA and RHA blended ECC



to the high water demand induced by the inclusion of 20%–55% RHA in ECC. Replacing a significant percentage of cement with RHA in ECC results in a decrease in water content in the mix, which affects the interfacial bond between fibres and cement matrix. Consequently, it weakens the load transfer between the fibres and matrix, ultimately leading to a decrease in flexural strength [18]. Hence, these properties remain almost equal at all testing ages until the ratio of fibres and other materials were increased or decreased. This is because a lower percentage of cement and w/c ratio impacts the flexural strength of mixes 20RHA to 55RHA at all ages of testing. Although the influence of M-sand on the bonding strength is unknown, it is widely known that silica sand moderately strengthens the binding of cementitious composites with PVA fibres [32]. According to the results, it is predicted that M-sand is a little more efficient than silica sand at improving the bonding strength between the fibre and matrix. The larger size (4.75 mm max) and rough surface of the M-sand can improve the bridging ability of the fibre compared to silica sand, whereas silica sand has a smaller size (50 μm to 300 μm) and a smooth surface area. All mixes reached a flexural strength above

16 MPa, which means that composites that achieve conformance may be created while effectively using M-sand and agricultural by-products.

6.2.4 Energy absorption

Figure 8 shows the impact strength of the different ECC mixes in terms of energy absorption at ultimate failure. The impact strength was improved with the replacement of cement by 10% to 30% BA and 10% to 40% RHA. Compared with CM 0.36, the impact energies of 10BA, 20BA, and 30BA increased to 54.230%, 68.32%, and 79.03%, respectively. Similarly, the mixes 10RHA, 20RHA, 30RHA, and 40RHA were significantly increased to 49.9%, 80.04%, 92.02%, and 108.1%, respectively, compared to CM 0.37. Compared with CC, the ductility of ECC is very high because of the elimination of coarse aggregates and the addition of fibres with better tensile (1600 MPa), elastic modulus (42.8 GPa), and elongation (6%) properties. According to Lin et al. [33] the impact resistance of PVA fibre was higher compared to other fibres, which can improve the impact strength of ECC. In addition, the multiple micro-cracking behaviors of ECC arrest

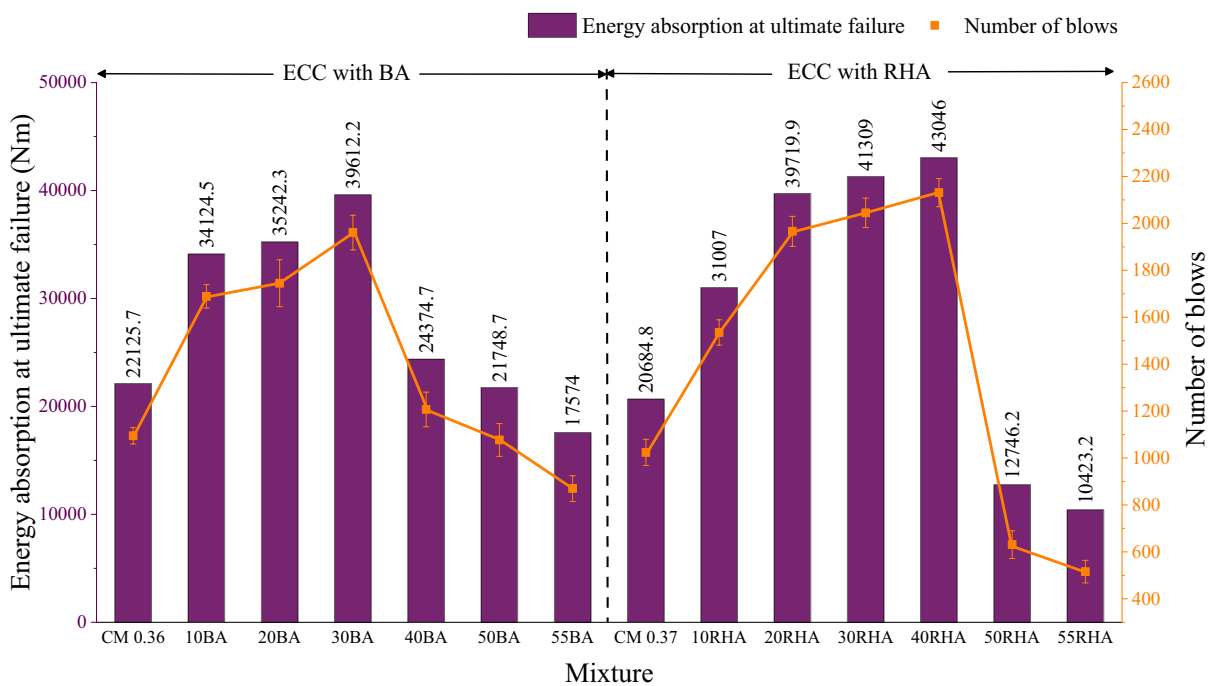


Fig. 8 Impact strength of BA and RHA blended ECC

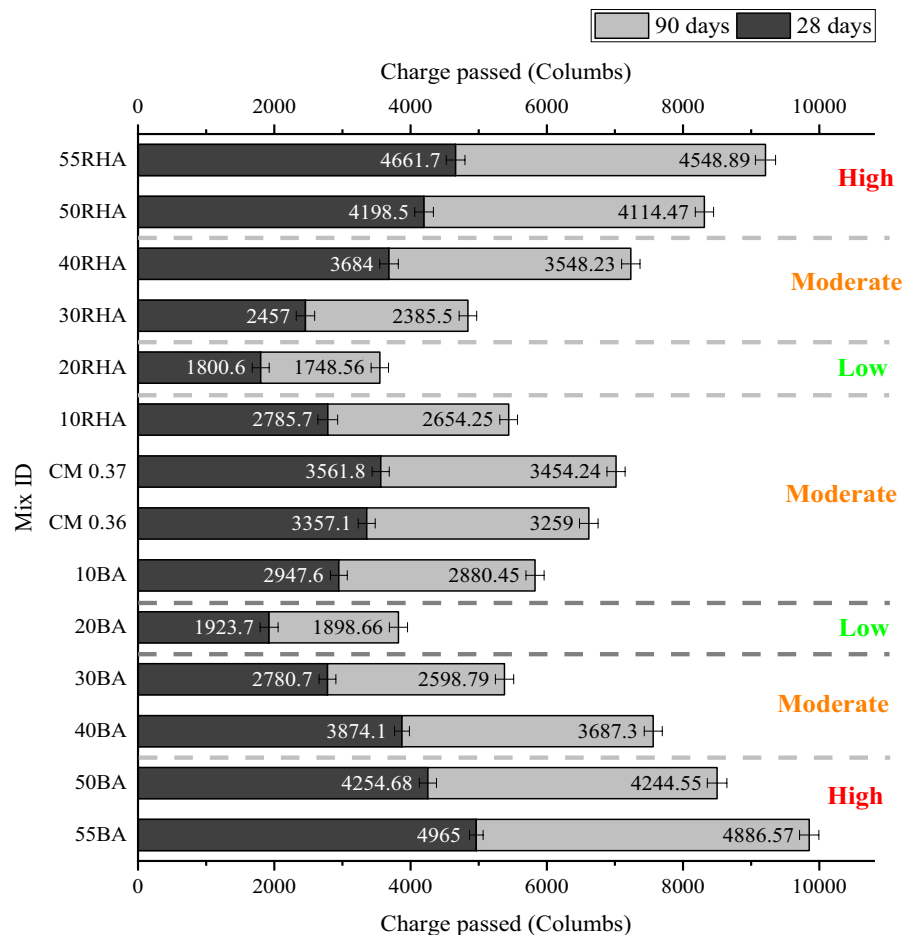
crack development and improve the bridging properties of ECC under impact loading. Nevertheless, the impact energy suddenly weakened owing to the dilution effect in the 40BA, 50BA, 55BA, 50RHA, and 55RHA compared to the corresponding control mixes. The minimum impact energy was observed as 17,574 Nm and 10,423.2 Nm in mixes 50BA and 55RHA, respectively, which were comparatively very high compared to conventional concrete. The impact energy of all ECC specimens consumed more energy absorption even after the formation of several micro-cracks owing to the high fibre bridging properties of the fibre and matrix [34]. From the overall findings, the ECC specimens performed outstanding in impact strength due to the positive outcome of fibres on the crack formation. Hence, ECC is more suitable for various impact resistance applications.

6.3 Durability property

6.3.1 Rapid chloride permeability

The chloride permeability of the BA and RHA blended ECC at the age of 28 and 90 days is illustrated in Fig. 9. In which, 20BA exhibited less chloride penetration of 1923.7 C and 1898.66 C at the age of 28 and 90 days, respectively, which are 42.70% and 41.74% lesser than CM 0.36. As discussed in Sect. 3, the presence of smaller particles in the BA increased the effectiveness of packing for the 10BA and 20BA mixes. As a result, the gaps between the larger particles decreased and the overall efficiency of the composites increased, thereby decreasing chloride penetration. However, chloride penetration was adversely affected when the percentage of BA increased by more than 20%. It increased from 2780.7 C to 4965 C and 2598.79 C to 4886.57 C while replacing OPC

Fig. 9 Chloride permeability of BA and RHA blended ECC



with BA increased from 30 to 55% at the age of 28 and 90 days, respectively. From the investigation, the penetration of chloride in 90 days specimens slightly improved over 28 days owing to the continued development of secondary C-S-H gel, as discussed in Sect. 6.2.2. In addition, the incorporation of M-Sand and BA with better particle size enhances the pore structure of 10BA and 20BA compared to conventional silica sand and fly ash. Hence, these finer pores created a more tortuous path for chloride ions, making it more difficult to penetrate the composites. On the other side, high amount of BA decreases the density and enhances the porosity in the ECC matrix owing to the lower specific gravity of BA than that of OPC. This decreased density and high porosity resulted in a lower compressive strength and increased chloride penetration in the ECC matrix. Similarly, the lower cement content and reduced pozzolanic activity of mixes 30BA, 40BA, 50BA, and 55BA adversely affect the penetration of the composites.

A similar result was observed by Chi et.al [35], where the charges decreased with increasing BA up to 20%. Increasing the percentage of RHA from 10 to 20, the chloride penetration was decreased by 2785.70 C and 1800.60 C, respectively, compared to CM 0.37 (3561.80 C) at the age of 28 days. Similarly, the 90 days chloride penetration decreased by 2654.25 C 1748.56 C compared to CM 0.37 (3454.24 C). This suggests that the addition of RHA likely alters the tortuosity of the capillary pores and refines them. The RHA particles filled the large capillary spaces by producing secondary hydration products, which refined the pore shape [26]. The minimum and maximum charge passed to the 28 days samples of about 1800.60 C and 4661.70 C, respectively, to the 90 days samples of about 1748.56 C and 4548.89 C, respectively. According to ASTM C 1202, the mixes CM

0.37, 10RHA, 30RHA, and 40RHA exhibited moderate penetration (2000–4000 coulombs), and 50RHA and 55RHA exhibited high penetration (greater than 4000 coulombs). The incorporation of more than 30% RHA in the ECC enlarged the porosity of the mixes, which creates a path for chloride penetration, thereby increasing the charges in mixes 30RHA to 55RHA. In addition, RHA requires high water content in the mixture for proper dispersion. This elevated water content leads to a higher w/cm ratio, increasing the capillary porosity and rendering the ECC more susceptible to chloride penetration. RHA has finer particles and a higher specific surface area than BA, as shown in Fig. 1 and Table 1. This finer particle size and a slightly higher w/cm ratio (0.37) improve the dispersion within the cementitious matrix, leading to a more effective pozzolanic reaction and resulting in a denser microstructure. Additionally, the high concentration of SiO₂ (95.85%) in RHA can facilitate the formation of a dense and impermeable hydration product, thereby reducing chloride ion permeability in the mixture [26]. According to Zhu et al., (2021) [36], the shrinkage of the ECC with above 30% of RHA mixes can increase the number of fibrous particles with more voids. This high shrinkage leads to the development of cracks within the matrix. These cracks create direct pathways for chloride ions to penetrate the composites, as chloride ions can easily move through open cracks.

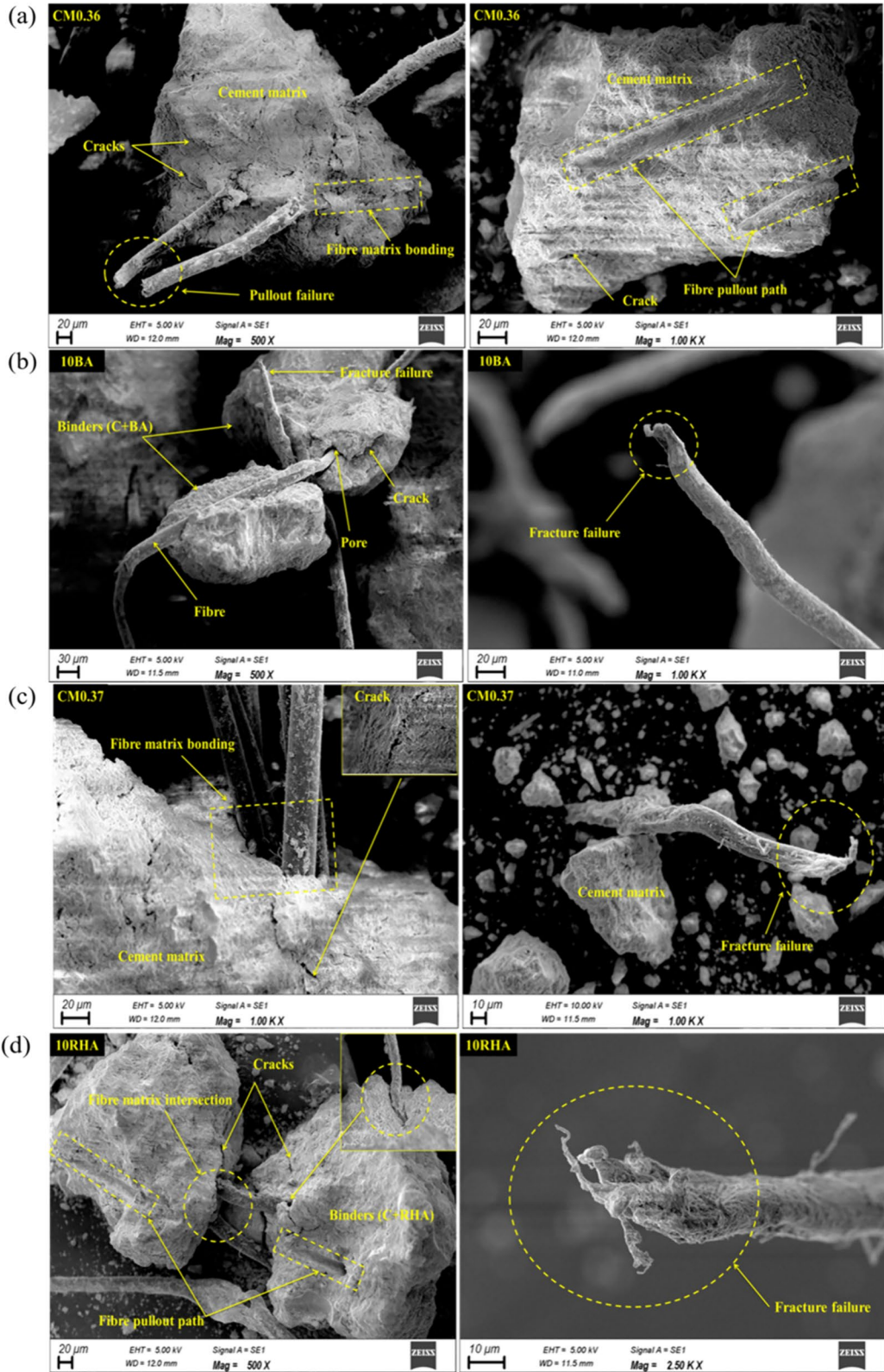
6.4 Cost analysis

The correlation between conventional ECC (i.e., ECC with FA and silica sand) and MECC (i.e., ECC with BA and RHA) is listed in Table 5 in terms of mechanical properties and cost analysis. According to V.C.Li [37] and Hao-Liang Wu [38] the physical properties

Table 5 Correlation between conventional and sustainable ECC

Properties / Mixtures	ECC with Fly Ash [37, 38] (55FA)	ECC with BA (55BA)	ECC with RHA (55RHA)
Cement to binder ratio	1:1.2	1:1.2	1:1.2
Compressive strength (MPa)	63.4	40.68	32.71
Firest cracking strength (MPa)	4.11 ± 0.66	0.825 ± 0.47	0.645 ± 0.47
Max tensile strength (MPa)	4.86 ± 0.47	1.193 ± 0.47	1.099 ± 0.41
Max tensile strain (%)	2.49 ± 0.57	2.003 ± 0.22	2.543 ± 0.14
Cost (USD/m ³)	443	398	398





◀**Fig. 10** Failure mode and bonding of fibres for different mixtures **a** 0.36, **b** 10BA, **c** 0.37 and **d** 10RHA

of conventional ECC are slightly better than those of ECC with BA and RHA. Nevertheless, the physical properties of the BA and RHA-based ECC were remarkably better than those of conventional concrete (CC) and Fibre reinforced concrete (FRC). In particular, the ductility of the ECC blended with RHA was higher than that of conventional ECC and FRC. However, the cost of the newly developed ECC (USD/m³) in this research is almost 10.158% less than that of conventional ECC owing to the replacement of silica sand and FA. Also, the effective use of agricultural by-products in ECC can reduce the carbon footprints; therefore, based on the research outcomes the ECC blended with BA, and RHA can be used for different civil engineering applications instead of FRC and CC.

6.5 Microstructure analysis

6.5.1 SEM analysis

The SEM are conducted for both control and optimal mixtures to identify the failure modes and bonding of fibres on cementitious composites, which are illustrated in Fig. 10. The fibres were entirely coated in cementitious composites without any fibre surface, which demonstrates that the PVA fibres had a strong hydrophilic connection and substantial bonding strength with binders. A thick slurry "protective shell" of cementing ingredients was developed on the surface of the PVA fibre, which exhibited a better bonding strength with the composites, thereby dissipating greater energy during the pull-out and fracture processes [39]. Nevertheless, cracks were observed in the binders in all mixtures because of the pull-out of the fibres. The cement matrix is weakened by fibre pullout, which causes the development of cracks in the entire composite [40]. The bonding zone between the cement matrix and fibres was formed in a cementitious system with numerous randomly dispersed microcracks during the testing stage. Furthermore, these microscopic or internal cracks started to develop after the pores proceeded to connect with one another. The microcracks and capillary energy quickly grew after the ultimate stress was achieved. These cracks began to appear during the loading phase, first at the bonding zone and subsequently at

the interface between the cement matrix and fibres. The microcracks and capillary energy grew rapidly after the ultimate stress was achieved. However, it started to decrease in the unloading phase after reaching the ultimate stress and thereby interconnected the microcracks in the cement matrix [41].

Compared to CM 0.36, the fibre fracture failure occurred primarily in the mixture 10BA, it was higher bonding between the fibre and cementitious composites. As discussed in Sect. 3, the existence of elongated and irregular particles in the BA improved the strong bond between the cement matrix and fibres. In contrast, both fracture and pull-out failure of fibres occurred in the mix 10RHA, which can reduce the ductility of the composites [42]. The bonding of the RHA mixed sample and PVA fibres was weakened owing to the existence of a large number of rounded particles. Additionally, pores were developed in the fibre matrix bonding zone owing to the pull-out of the fibre, which weakened the cement mortar and propagated the cracks in the cement matrix.

7 Conclusion and recommendation

This study examined the influence of different percentages of BA and RHA along with M-sand on fresh and hardened properties of modified ECC. The experimental results led to the following conclusions:

- The flowability of ECC was significantly reduced by replacing OPC with different percentages of BA and RHA. Especially, increasing the RHA percentage from 0 to 55 the flow significantly decreases the flow from 92.5% to 69%. Whereas, the flowability of ECC with BA reached 91.2% to 77.8% owing to the presence of high quantities of rounded particles. The 3 and 7 days compressive strength of the BA-blended ECC were lower than those of CM 0.36. However, it increased at 28 days from 53.14 MPa to 54.12 MPa owing to presence of high silica content in BA which increases the secondary hydration process. Also, ECC with 10% BA attained optimal strength compared to the other mixes blended with BA. Similarly, ECC with 10% RHA exhibited maximum strength at 3, 7, and 28 days. The minimum strength of ECC with 55% of BA, and 55%

of RHA attained 40.68 MPa and 32.71 MPa at 28 days.

- ECC with the addition of 10% BA and 10% RHA exhibited a high direct tensile strength of 2.82 MPa and 2.39 MPa, respectively, at 28 days. The ductility of ECC with 40% BA and 10% RHA reached maximum values of 3.0981% and 3.7320%, respectively. Also, high amounts of BA (55%) and RHA (55%) exhibited tensile strains of 2.003% and 2.543%, which are much higher than those of conventional concrete. The flexural strengths of all mixtures exhibited a similar trend of compressive strength, where the flexural strength of 10BA was 17.169%, 6.53%, and 5.679% higher than CM 0.36 at 3, 7, and 28 days, respectively. Correspondingly, 10RHA attained high percentages of 18.19, 23.5 and 22.80 compared to CM 0.37. Compared to the RHA mixtures, the ECC-blended BA exhibited high flexural strength at all testing ages. Also, 30BA and 40BA mixtures exhibited high impact energy at 28 days owing to the high physical properties and diffusion of the fibres.
- The durability characteristics of the BA and RHA-blended ECC mixes significantly improved when the OPC was replaced by 20%. The chloride penetration for the 20BA mix reached 1923.7 C at the age of 28 days and 1898.66 C at 90 days, attributed to the smaller particles in BA increasing the packing effectiveness. The morphology results agree with the mechanical properties of the MECC. In addition, the cost of MECC was 10.158% lesser than that of conventional ECC because of the replacement of silica sand and fly ash.

Acknowledgements The authors wish to thank Dr. K Prakasan, Principal, PSG College of Technology, Coimbatore, for the facilities and support provided for carrying out this research at Advanced Concrete Research Laboratory.

Author contributions N. Shanmugasundaram: Conceptualization, Methodology, Investigation, and Writing an original draft. S. Praveenkumar: Writing—review & editing, Supervision.

Data availability The authors declare that the data supporting the findings of this study are available within the article.

Declarations



Conflict of interest The authors declare that they have no known competing financial interests or personal relationships that could have appeared to influence the work reported in this paper.

References

1. Abbas AN, Al-Nealy H, Al-Saadi A, Imran M (2020) The effect of using sugar-cane bagasse ash as a cement replacement on the mechanical characteristics of concrete. *Mater Sci Forum* 1002(2001):565–577. <https://doi.org/10.4028/www.scientific.net/MSF.1002.565>
2. Miyandehi BM, Feizbakhsh A, Yazdi MA, Liu QF, Yang J, Alipour P (2016) Performance and properties of mortar mixed with nano-CuO and rice husk ash. *Cem Concr Compos* 74:225–235. <https://doi.org/10.1016/j.cemconcomp.2016.10.006>
3. Bahurudeen A, Kanraj D, Dev VG, Santhanam M (2015) Performance evaluation of sugarcane bagasse ash blended cement in concrete. *Cem Concr Compos* 59:77–88. <https://doi.org/10.1016/j.cemconcomp.2015.03.004>
4. Ashraf M et al (2022) Developing a sustainable concrete incorporating bentonite clay and silica fume: Mechanical and durability performance. *J Clean Prod* 337:130315. <https://doi.org/10.1016/j.jclepro.2021.130315>
5. Ganesan K, Rajagopal K, Thangavel K (2007) Evaluation of bagasse ash as supplementary cementitious material. *Cem Concr Compos* 29(6):515–524. <https://doi.org/10.1016/j.cemconcomp.2007.03.001>
6. Divya S et al (2024) Pozzolanic attributes of hydraulic cement paste hybridized with agricultural by-product and Nano-carbon. *Constr Build Mater* 411:134119. <https://doi.org/10.1016/j.conbuildmat.2023.134119>
7. Park KB, Kwon SJ, Wang XY (2016) Analysis of the effects of rice husk ash on the hydration of cementitious materials. *Constr Build Mater* 105:196–205. <https://doi.org/10.1016/j.conbuildmat.2015.12.086>
8. Shanmugasundaram N, Praveenkumar S (2023) Adhesive characteristics of novel greener engineered cementitious composite with conventional concrete substrate. *Constr Build Mater* 407:133591. <https://doi.org/10.1016/j.conbuildmat.2023.133591>
9. Hariaravind G et al (2023) Behaviour of FRP-ECC-HSC composite stub columns under axial compression : Experimental and mathematical approach concrete filled steel tubular columns. *Constr Build Mater* 408:133707
10. MN Uddin et al., (2024) Prediction of compressive strength and tensile strain of engineered cementitious composite using machine learning, no. 0123456789. Springer Netherlands,.
11. Divya S et al (2024) Harden and self-sensing properties of engineered cementitious composite reinforced with nano-carbon. *IGI Glob*. <https://doi.org/10.4018/978-1-6684-8182-0.ch004>
12. Shanmugasundaram N et al (2022) Prediction on compressive strength of engineered cementitious composites using machine learning approach. *Constr Build Mater*

- 342:127933. <https://doi.org/10.1016/j.conbuildmat.2022.127933>
13. Tosun-Felekoğlu K, Gödek E, Keskinateş M, Felekoğlu B (2017) Utilization and selection of proper fly ash in cost effective green HTPP-ECC design. *J Clean Prod* 149:557–568. <https://doi.org/10.1016/j.jclepro.2017.02.117>
 14. Shoji D, He Z, Zhang D, Li VC (2022) The greening of engineered cementitious composites (ECC): A review. *Constr Build Mater* 327:126701. <https://doi.org/10.1016/j.conbuildmat.2022.126701>
 15. Subedi S, Arce G, Hassan MM, Mohammad LN (2021). Feasibility of Engineered cementitious composites implementing combined systems of post-processed bagasse ash and fly ash as SCMs. In *Tran-SET 2021* (pp. 353-364). Reston, VA: American Society of Civil Engineers.
 16. Subedi S, Arce GA, Hassan MM, Barbato M, Mohammad LN, Rupnow T (2022) Feasibility of ECC with high contents of post-processed bagasse ash as partial cement replacement. *Constr Build Mater* 319:126023. <https://doi.org/10.1016/j.conbuildmat.2021.126023>
 17. Amin MN et al (2020) Role of sugarcane bagasse ash in developing sustainable engineered cementitious composites. *Front Mater* 7:65. <https://doi.org/10.3389/fmats.2020.00065>
 18. Zhang Z, Yang F, Liu JC, Wang S (2020) Eco-friendly high strength, high ductility engineered cementitious composites (ECC) with substitution of fly ash by rice husk ash. *Cem Concr Res* 137:106200. <https://doi.org/10.1016/j.cemconres.2020.106200>
 19. Zhou Y, Zheng S, Huang X, Xi B, Huang Z, Guo M (2021) Performance enhancement of green high-ductility engineered cementitious composites by nano-silica incorporation. *Constr Build Mater* 281:122618. <https://doi.org/10.1016/j.conbuildmat.2021.122618>
 20. Shanmugasundaram N, Praveenkumar S (2023) Influence of manufactured sand gradation and water cement ratios on compressive strength of engineered cementitious composites. *Mater Today Proc.* <https://doi.org/10.1016/j.matpr.2023.05.024>
 21. Memon SA, Javed U, Shah MI, Hanif A (2022) Use of processed sugarcane bagasse ash in concrete as partial replacement of cement: mechanical and durability properties. *Buildings* 12(10):1–18. <https://doi.org/10.3390/buildings12101769>
 22. Ajith G et al (2021) Effect of mineral admixtures and manufactured sand on compressive strength of engineered cementitious composite. *J Build Pathol Rehabil* 6(1):1–9. <https://doi.org/10.1007/s41024-021-00137-y>
 23. Shanmugasundaram N, Praveenkumar S (2022) Mechanical properties of engineered cementitious composites (ECC) incorporating different mineral admixtures and fibre: a review. *J Build Pathol Rehabil* 7(1):40. <https://doi.org/10.1007/s41024-022-00182-1>
 24. Shanmugasundaram N, Praveenkumar S (2021) Influence of supplementary cementitious materials, curing conditions and mixing ratios on fresh and mechanical properties of engineered cementitious composites – A review. *Constr Build Mater* 309:125038. <https://doi.org/10.1016/j.conbuildmat.2021.125038>
 25. Hanif Khan M, Zhu H, Ali Sikandar M, Zamin B, Ahmad M, Sabri MS, M. (2022) Effects of various mineral admixtures and fibrillated polypropylene fibers on the properties of engineered cementitious composite (ECC) based mortars. *Materials* 15(8):2880. <https://doi.org/10.3390/ma15082880>
 26. Da Costa FBP, Righi DP, Graeff AG, da Silva Filho LCP (2019) Experimental study of some durability properties of ECC with a more environmentally sustainable rice husk ash and high tenacity polypropylene fibers. *Constr Build Mater* 213:505–513. <https://doi.org/10.1016/j.conbuildmat.2019.04.092>
 27. Zhang Z, Li Z, He J, Shi X (2023) High-strength engineered cementitious composites with nanosilica incorporated: mechanical performance and autogenous self-healing behavior. *Cem Concr Compos* 135:104837. <https://doi.org/10.1016/j.cemconcomp.2022.104837>
 28. Tahmouresi B, Nemati P, Asadi MA, Saradar A, Moein MM (2021) Mechanical strength and microstructure of engineered cementitious composites: a new configuration for direct tensile strength, experimental and numerical analysis. *Constr Build Mater* 269:121361. <https://doi.org/10.1016/j.conbuildmat.2020.121361>
 29. Fu C, Chen M, Guo R, Qi R (2022) Green-engineered cementitious composite production with high-strength synthetic fiber and aggregate replacement. *Materials* 15(9):3047. <https://doi.org/10.3390/ma15093047>
 30. Yücel HE, Öz HÖ, Güneş M, Kaya Y (2021) Rheological properties, strength characteristics and flexural performances of engineered cementitious composites incorporating synthetic wollastonite microfibers with two different high aspect ratios. *Constr Build Mater* 306:124921. <https://doi.org/10.1016/j.conbuildmat.2021.124921>
 31. Li M, Li VC (2011) High-early-strength engineered cementitious composites for fast, durable concrete repair-material properties. *ACI Mater J* 108(1):3–12. <https://doi.org/10.14359/51664210>
 32. Li VC, Wang S, Wu C (2001) Tensile strain-hardening behavior of polyvinyl alcohol engineered cementitious composite (PVA-ECC). *ACI Mater J* 98(6):483–492. <https://doi.org/10.14359/10851>
 33. Lin JX et al (2020) Static and dynamic mechanical behavior of engineered cementitious composites with PP and PVA fibers. *J Build Eng* 29:101097. <https://doi.org/10.1016/j.jobbe.2019.101097>
 34. Hu S, Cai H, Hong R, Li M, Yao F (2021) Performance test and microstructure of modified PVC aggregate-hybrid fiber reinforced engineering cementitious composite (ECC). *Materials (Basel)* 14(8):1856. <https://doi.org/10.3390/ma14081856>
 35. Chi MC (2012) Effects of sugar cane bagasse ash as a cement replacement on properties of mortars. *Sci Eng Compos Mater* 19(3):279–285. <https://doi.org/10.1515/secm-2012-0014>
 36. Zhu JX, Xu LY, Huang BT, Weng KF, Dai JG (2022) Recent developments in engineered/strain-hardening cementitious composites (ECC/SHCC) with high and ultra-high strength. *Constr Build Mater* 342:127956. <https://doi.org/10.1016/j.conbuildmat.2022.127956>
 37. Wang S, Li VC (2007) Engineered cementitious composites with high-volume fly ash. *ACI Mater J* 104(3):233–241. <https://doi.org/10.14359/18668>



38. Wu HL, Zhang D, Ellis BR, Li VC (2018) Development of reactive MgO-based Engineered Cementitious Composite (ECC) through accelerated carbonation curing. *Constr Build Mater* 191:23–31. <https://doi.org/10.1016/j.conbuildmat.2018.09.196>
39. Zhang D, Yang W, Ge Y, Liu P (2022) Study on fine-tuned fly ash content for lightweight strain-hardening cementitious composites (LSHCC) with low fiber content. *Constr Build Mater* 347:128333. <https://doi.org/10.1016/j.conbuildmat.2022.128333>
40. Yao Q, Teng X, Lu C, Sun H, Mo J, Chen Z (2023) Influence of accelerated chloride corrosion on mechanical properties of sea sand ECC and damage evaluation method based on nondestructive testing. *J Build Eng* 63:105520. <https://doi.org/10.1016/j.jobe.2022.105520>
41. Hu S, Cai H, Yuan Z, Cheng L (2022) Performance comparison test of new sprayed engineered cementitious composites and C25 sprayed concrete. *Case Stud Constr Mater* 16:e01139. <https://doi.org/10.1016/j.cscm.2022.e01139>
42. Gao S, Ban S, Wang H, Lei D, Gong Y (2022) The influence of oiled fiber, freeze-thawing cycle, and sulfate attack on strain hardening cement-based composites. *Rev*

Adv Mater Sci 61(1):208–220. <https://doi.org/10.1515/rams-2022-0023>

Publisher's Note Springer Nature remains neutral with regard to jurisdictional claims in published maps and institutional affiliations.

Springer Nature or its licensor (e.g. a society or other partner) holds exclusive rights to this article under a publishing agreement with the author(s) or other rightsholder(s); author self-archiving of the accepted manuscript version of this article is solely governed by the terms of such publishing agreement and applicable law.

